Phenotyping Rodent Models of Obesity by MRI

Thesis Defense, May 22, 2009

David Johnson

Obesity

- A costly, growing epidemic ($51 billion in 1995 as per Wolf et al.)
- Linked with diabetes, high blood pressure, and dyslipidemia
- Both genetic and environmental factors are significant

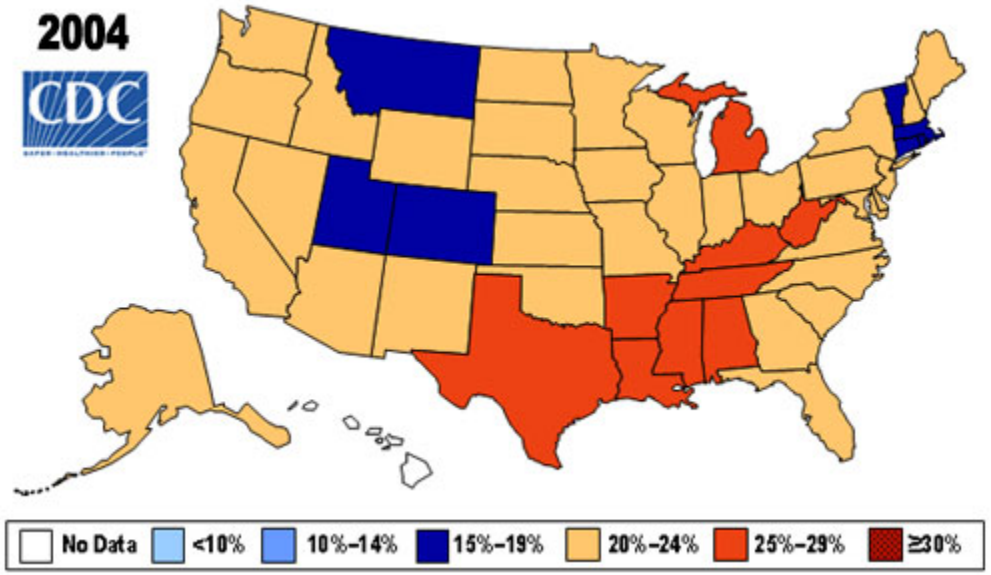

BMI>30, CDC Behavioral Risk Factor Surveillance System

Ohio BMI>30

2007	28.1%
1997	17.7%

Obesity: Genes and Environment

Genes

- Android vs. gynoid body shapes
- 300+ possible quantitative trait loci
- Links to specific fat depots

Environment

- Diet
- Exercise
- Related diseases and therapies

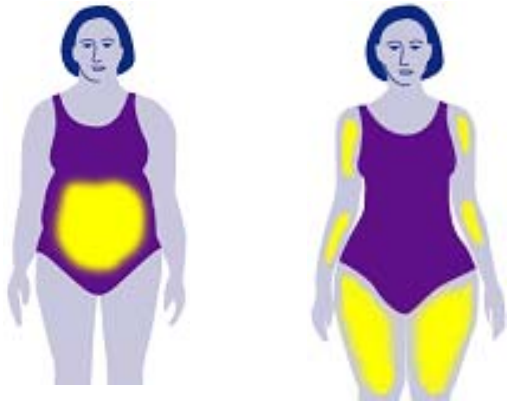

Android Gynoid

Why use rats and mice to study diseases linked to human obesity?

- Cost / sample size
- Patient compliance
- Uniform genetic background
- Genetic engineering possible
- FDA requirements for drug approval

Magnetic Resonance Imaging (MRI) of Obesity

- Why use MRI to study obesity?
  - Excellent soft tissue contrast
  - Non-invasive, no ionizing radiation
  - Acquisition and image processing techniques can be translated from MRI systems designed for rodents to systems designed for humans

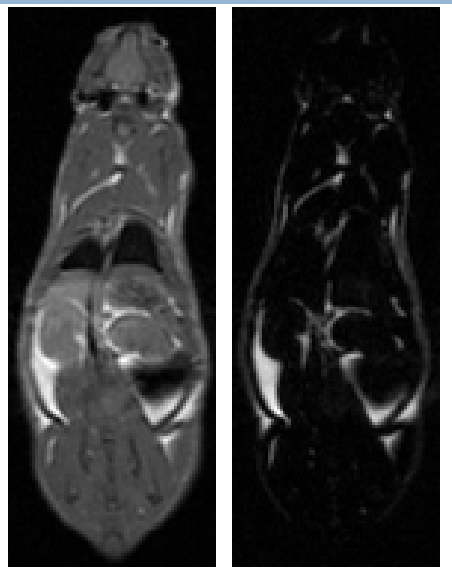

T1W CHESS

Specific Aims

- Thesis: ratio imaging is a robust image analysis technique for phenotyping rodent models of obesity using MRI
- Developing the ratio imaging technique for phenotyping rats on a clinical MRI
  - Aim 1: Semiautomatic ratio image analysis
- Modifying the technique for high field phenotyping of mice
  - Aim 2: Robust IDEAL reconstruction on a graphics card
- Validating the high field measurements using a mouse model of dietary obesity
  - Aim 3: IDEAL Mouse Imaging at 7T

The big picture

- How do we turn images into measurements and phenotypes?

Input Image

Image Processing →

Quantitative Output Image

Tissue volumes, fat concentrations

Aim 1: Semiautomatic ratio image analysis

A. Developing a robust image analysis technique
   i. Enable rapid phenotyping via ratio imaging
   ii. Remove signal intensity dependence on position in receiver coil, T1 and T2, and the spatial chemical shift artifact
   iii. Reduce inter-operator variability in tracing abdominal fat

B. Validation using SHR/SHROB rat model
   i. Identify MRI phenotypes of both genetic and dietary induced obesity via subcutaneous and visceral fat depot volumes
   ii. Also test for liver fat concentration differences

i. Semi-automatic segmentation

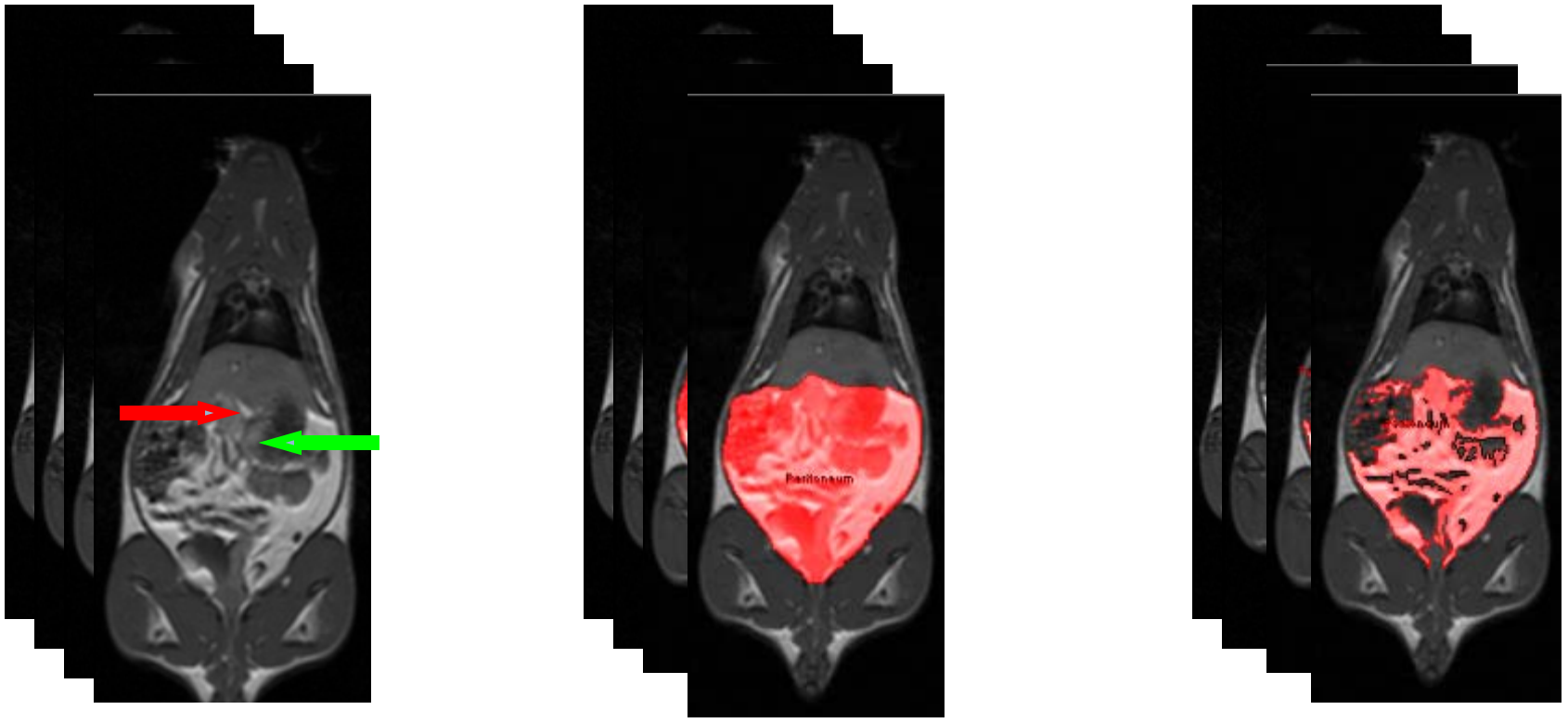

Measure visceral fat in the abdomen by tracing the abdominal wall (peritoneum) and then applying a threshold.

i. Coil Sensitivity Inhomogeneity

- Coil inhomogeneity sensitivity in this image confounds analysis
  - Affects all images from MRI scanners
  - Not reproducible because animal will be positioned differently every time in the MRI
  - Difficult to apply thresholds to images

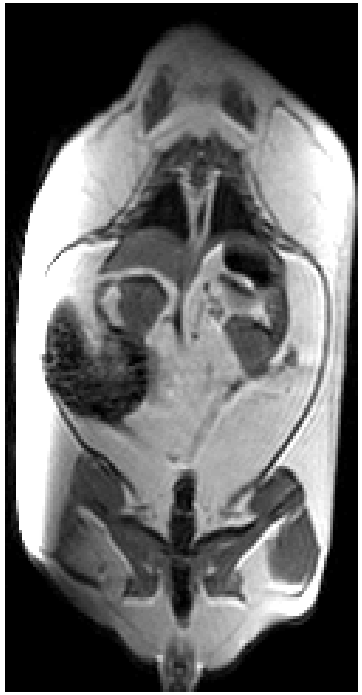

T1W

CHESS

ii. Ratio Image Math

$$I_r(x,y) = \frac{\rho_{0,F}(x,y)}{\rho_{0,F}(x,y) + \rho_{0,W}(x,y)} = \frac{\dfrac{I_F(x,y)}{[(1-e^{-TR/T1F})e^{-TE/T2F}]}}{\dfrac{I_F(x,y)}{[(1-e^{-TR/T1F})e^{-TE/T2F}]} + \dfrac{I_{FW}(x,y) - I_F(x,y)}{(1-e^{-TR/T1W})e^{-TE/T2W}}}$$

- This model incorporates the signal intensity in the unsaturated image (I_{FW}) with fat and water spin densities ($\rho_{0,F}$ and $\rho_{0,W}$), T1 and T2 relaxation effects for both water and fat (T1F, T2F, T1W, and T2W), and a spatially varying receiver coil sensitivity pattern, or bias field (Λ).

ii. Ratio Image

Fat only ÷ **Fat+Water** = **% Lipid**

CHESS **T1W** **Ratio Image**

- Apply T1 and T2 corrections
- Divide the two images

iii. Intra-operator variability

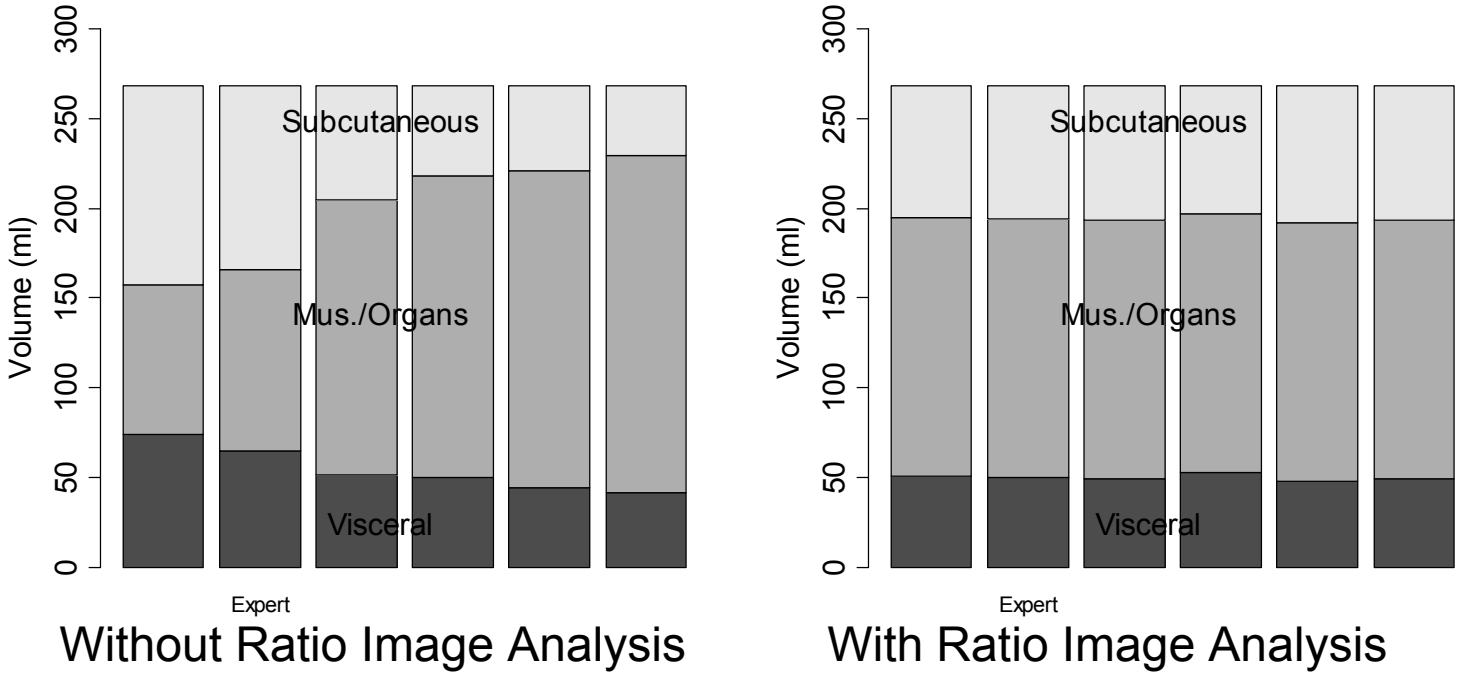

- Ratio image analysis removed differences in manual segmentation of the abdominal cavity.

iii. Scan-rescan Reproducibility

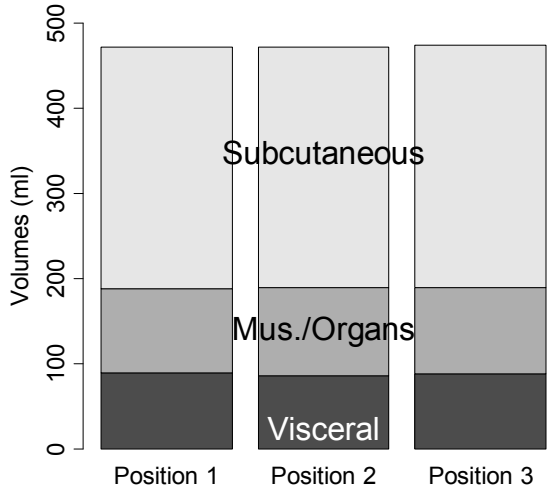

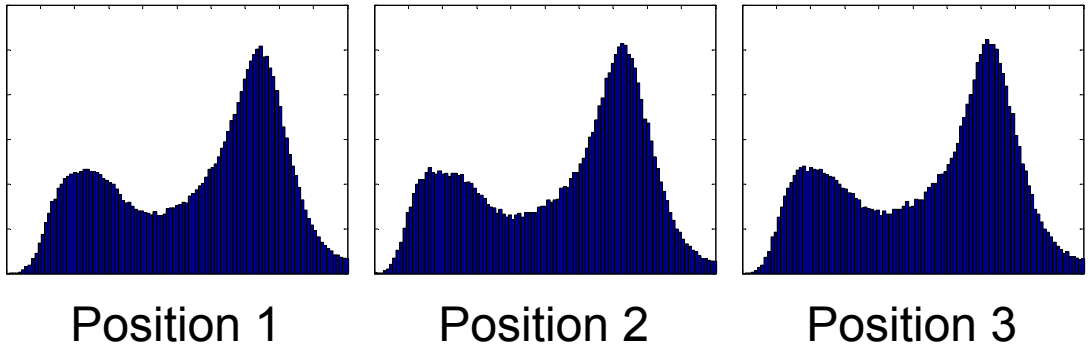

- Three separate acquisitions of the same SHROB rat showed no significant differences in measured visceral and subcutaneous adipose tissue volumes despite repositioning and reshimming (2% and 0.5% coefficients of variation, respectively).

B. Aim 1 Validation: SHR/SHROB Rat model of Metabolic Syndrome

SHR
294.5g

SHR-DO
427.5g

Insulin resistance
Hypertension
Dyslipidemia
Hyperglycemia

SHROB
529.5g

- Spontaneously Hypertensive Rat (SHR/Kol) – lean control rats
- Dietary obese SHR (SHR-DO) – SHR becomes obese on a milkshake supplemented diet
- Obese Spontaneously Hypertensive Rat (SHROB/Kol) – established model of Metabolic Syndrome

i. MRI Phenotypes in SHR/SHROB rats

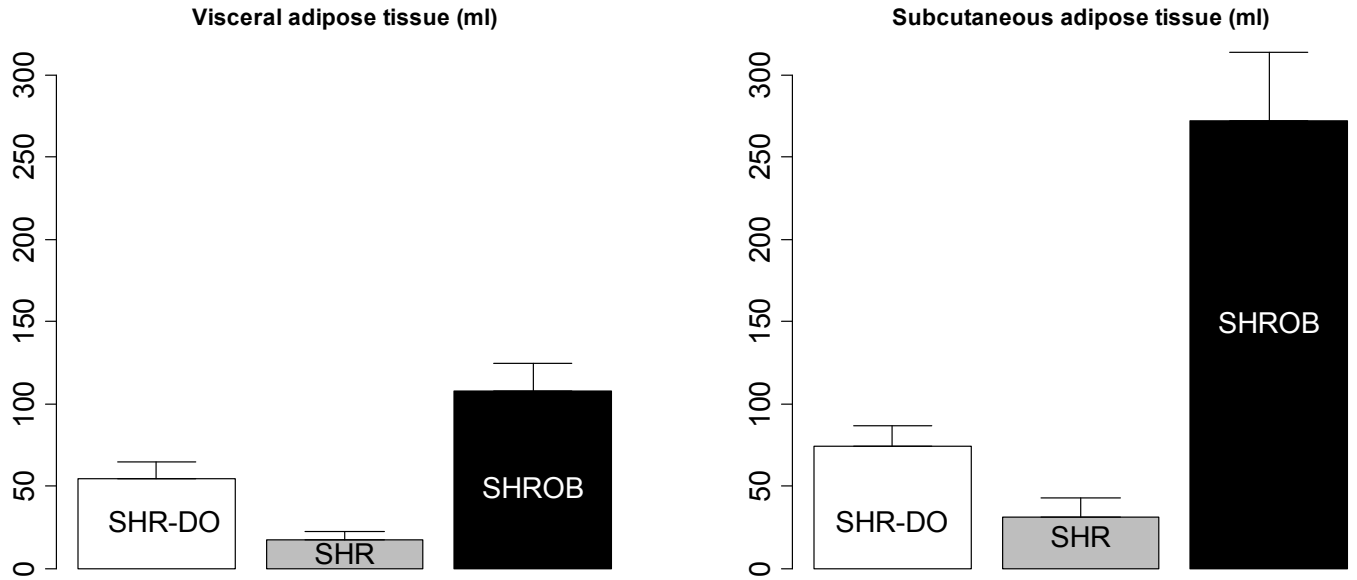

- Visceral adipose tissue is enlarged due to both dietary and genetic obesity ($P<0.01$ SHR-DO vs. SHR, and $P<0.01$ SHROB vs. SHR)
- But subcutaneous adipose tissue is enlarged only in dietary obesity ($P=0.07$ SHR-DO vs. SHR and $P<0.01$ SHROB vs. SHR)

ii. MRI Liver Phenotypes in SHR/SHROB rats

- Liver signal intensity in the ratio images showed a difference among SHROB rats (P<0.05 SHROB vs. SHROB*)
- SHR rats had less liver fat than SHR-DO or SHROB (P<0.05)
- Suggests that dietary and genetic obesity both contribute to liver fat

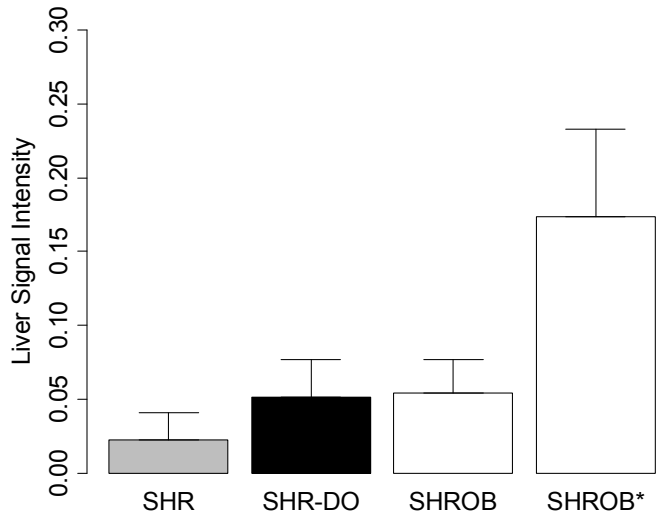

Aim 1: Conclusions

- A robust image analysis technique was developed
  - Signal intensity dependence on position in receiver coil, T1 and T2, and the spatial chemical shift artifact were removed
  - Measured tissue volumes were reproducible despite repositioning and reshimming
  - Inter-operator variability in tracing abdominal fat was eliminated
- The SHR/SHROB rat model demonstrated the utility and effectiveness of the technique
  - MRI phenotypes of both genetic and dietary induced obesity were identified with increased subcutaneous and visceral fat depot volumes
  - Differences in liver fat concentration were observed

Transition to High Field MRI

- Why use a MRI scanner designed specifically for small animals?
  - Better SNR, higher resolution images, faster acquisitions
  - Devoted to research
  - Able to image mice (lower costs, more genetic variants)
- Ratio image analysis still works
  - Same image analysis from fat and water images
- What new issues have to be addressed?
  - B_0 field inhomogeneity
  - Higher resolution images → more data → slower reconstruction

B_0 Field Inhomogeneity

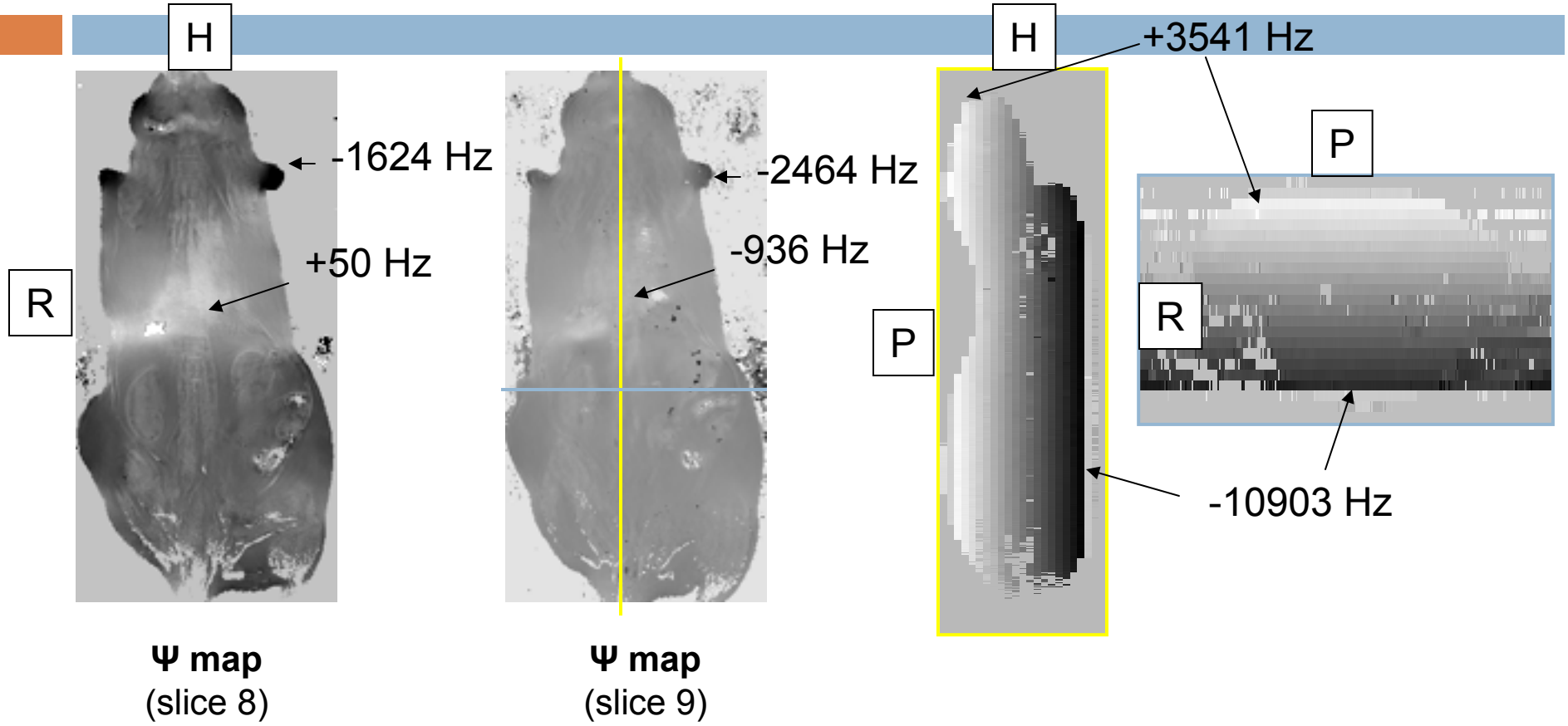

Ψ map
(slice 8)

Ψ map
(slice 9)

- Field inhomogeneity causes failures in CHESS saturation
- Much worse at 7T on small animal MRIs than on low field human systems

Dixon Imaging

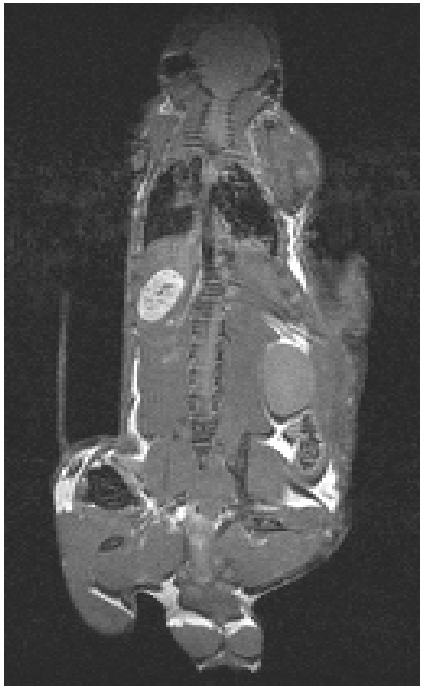

TE1=79 us

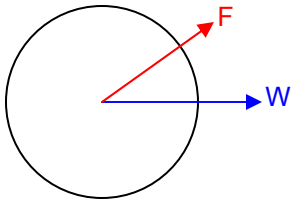

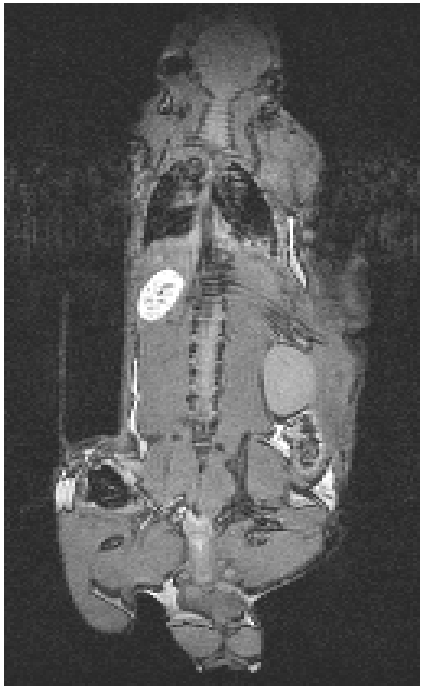

TE2=396 us

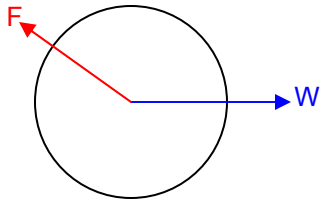

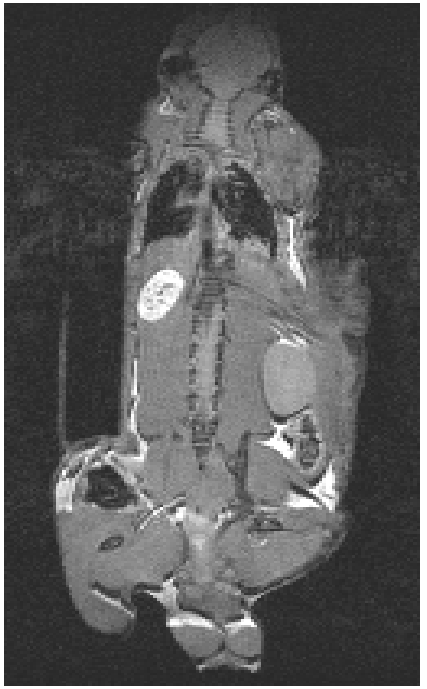

TE3=714 us

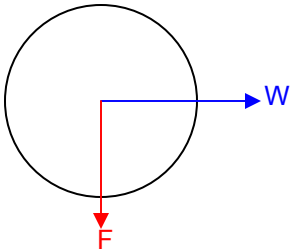

3 Point Dixon Math

$$s(TE) = \left(\rho_w + \rho_f e^{j2\pi\Delta f TE}\right) e^{j2\pi\gamma\Delta B_0 TE}$$

Assuming T2* decay is neglected

$$\begin{aligned} s(TE_1) &= \left(\rho_w + \rho_f\right) e^{j2\pi\gamma\Delta B_0 TE_1} \\ s(TE_2) &= \left(\rho_w - \rho_f\right) e^{j2\pi\gamma\Delta B_0 TE_2} \\ s(TE_3) &= \left(\rho_w + \rho_f\right) e^{j2\pi\gamma\Delta B_0 TE_3} \end{aligned}$$

Reconstruct

$$\gamma\Delta B_0 = \frac{1}{TE_3 - TE_1}\arg\left(\frac{s(TE_3)}{s(TE_1)}\right)$$

$$\rho_w = \frac{1}{2}\left(s(TE_1)e^{-j2\pi\gamma\Delta B_0 TE_1} + s(TE_2)e^{-j2\pi\gamma\Delta B_0 TE_2}\right)$$

$$\rho_f = \frac{1}{2}\left(s(TE_1)e^{-j2\pi\gamma\Delta B_0 TE_1} - s(TE_2)e^{-j2\pi\gamma\Delta B_0 TE_2}\right)$$

Caveat: phase unwrapping required in ΔB_0 and s(TE)

$$\underbrace{\begin{bmatrix} S(TE1) \\ S(TE2) \\ S(TE3) \end{bmatrix}}_{S(x,y)} = \underbrace{\begin{bmatrix} e^{j2\pi\gamma\Delta B_0 TE_1} & 0 & 0 \\ 0 & e^{j2\pi\gamma\Delta B_0 TE_2} & 0 \\ 0 & 0 & e^{j2\pi\gamma\Delta B_0 TE_3} \end{bmatrix}}_{\Psi(x,y)} \underbrace{\begin{bmatrix} 1 & 1 \\ 1 & -1 \\ 1 & 1 \end{bmatrix}}_{A} \underbrace{\begin{bmatrix} \rho_W \\ \rho_F \end{bmatrix}}_{\rho(x,y)}$$

Fat-Water Reconstruction

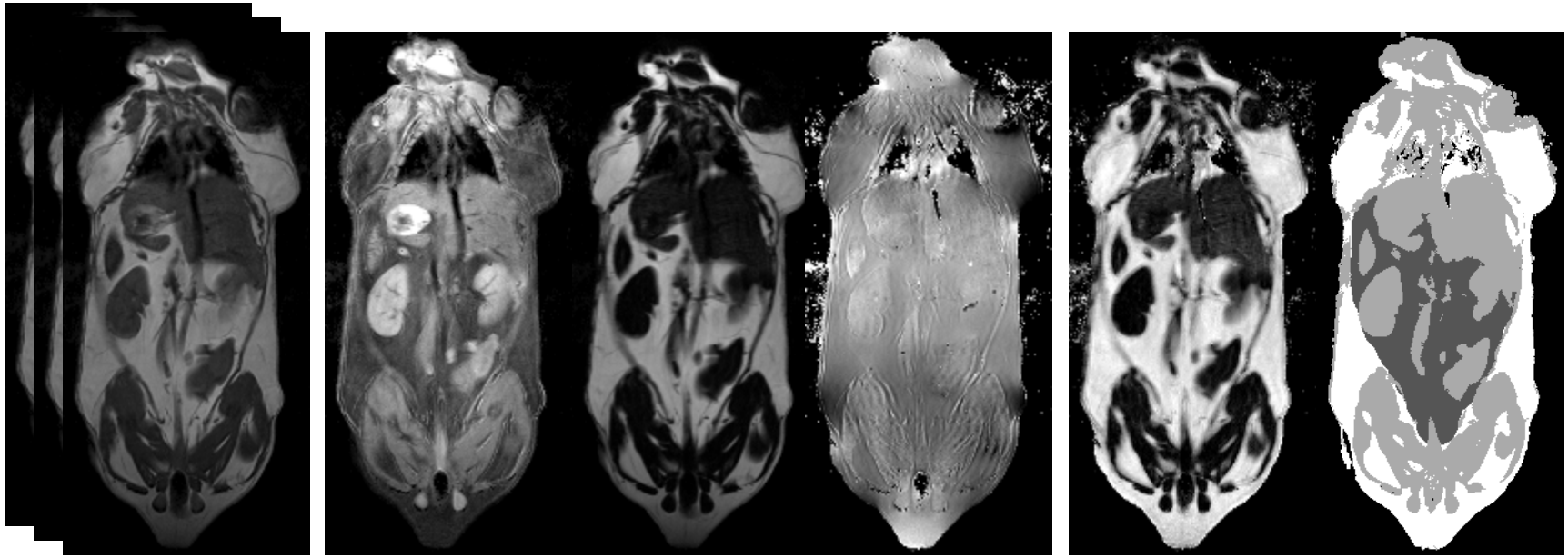

Input 3 images | **|W|** | **|F|** | **ψ** | **Ratio** | **Label Image**

Outputs

The ratio image |F|/|W+F| is used to measure tissue volumes as before

Aim #2: Robust IDEAL reconstruction on a graphics card

- Hypothesis: The processing speed and robustness of the IDEAL reconstruction can be improved
  i. Vectorize IDEAL equations for speed and for graphics card (GPU) computation
  ii. Use Brent's method instead of Golden Section Search to reduce the number of iterations of the optimization
  iii. Fix Ψ aliasing using weighted planar extrapolation

i. Graphics Cards: Your personal supercomputer

CalcUA (University of Antwerp):

- $5 million, built for CT reconstruction research in 2005
- Most powerful supercomputer in Belgium
- 256 AMD Opteron nodes (2 cores per node, 2.4GHz)

FASTRA (University of Antwerp):

- $10,000 in 2008
- Designed by graduate students
- 4 Nvidia 9800GX2 cards (128 cores per GPU, 2x GPUs, 1.5GHz)

- CalcUA can reconstruct a 1024x1024x1024 CT dataset in 67.4 s
- FASTRA can reconstruct the same data in 52.2 s
- Standard desktop PC takes at least 4 hours

Data from FASTRA's public release on their website, http://fastra.ua.ac.be

i. IDEAL Reconstruction

FOR each (x,y):

Iteratively minimize the residuals at pixel(x,y):

Identify 2 values of ψ: ψ_F (fat dominant), ψ_W (water dominant)

Pick the correct one based on spatial smoothness

$$\underbrace{\begin{bmatrix} S(TE1) \\ S(TE2) \\ S(TE3) \end{bmatrix}}_{S(x,y)} = \underbrace{\begin{bmatrix} e^{j2\pi\psi TE_1} & 0 & 0 \\ 0 & e^{j2\pi\psi TE_2} & 0 \\ 0 & 0 & e^{j2\pi\psi TE_3} \end{bmatrix}}_{\Psi(x,y)} \underbrace{\begin{bmatrix} 1 & e^{j2\pi\Delta f\, TE_1} \\ 1 & e^{j2\pi\Delta f\, TE_2} \\ 1 & e^{j2\pi\Delta f\, TE_3} \end{bmatrix}}_{A} \underbrace{\begin{bmatrix} \rho_W \\ \rho_F \end{bmatrix}}_{\rho(x,y)}$$

$$J(\psi) = \left\| \left(I - AA\dagger\right) \begin{bmatrix} \exp(-j2\pi\psi TE1) & 0 & 0 \\ 0 & \exp(-j2\pi\psi TE2) & 0 \\ 0 & 0 & \exp(-j2\pi\psi TE3) \end{bmatrix} \begin{bmatrix} S(TE1) \\ S(TE2) \\ S(TE3) \end{bmatrix} \right\|$$

Why are there two possible solutions for ψ? Consider a pixel with only one proton species.

$$S(TE) = W\exp(j2\pi\psi_W TE)$$

Equivalent

$$\begin{aligned} S(TE) &= (F\exp(j2\pi\Delta f TE))\exp(j2\pi\psi_F TE) \\ &= (F\exp(j2\pi\Delta f TE))\exp(j2\pi(\psi_W - \Delta f)TE) \\ &= W\exp(j2\pi\psi_W TE) \end{aligned}$$

$$\psi_1 = \psi_2 + \frac{1}{2\pi\Delta TE}\arg\left(\frac{W + F\exp(j2\pi\Delta f\,\Delta TE)}{F + W\exp(j2\pi\Delta f\,\Delta TE)}\right)$$ For any pixel where W≠F

i. Vectorized IDEAL

- Vectorization is required for GPU implementation

$$J(\psi) = \left\| \left(I - AA\dagger\right) \begin{bmatrix} \exp(-j2\pi\psi TE1) & 0 & 0 \\ 0 & \exp(-j2\pi\psi TE2) & 0 \\ 0 & 0 & \exp(-j2\pi\psi TE3) \end{bmatrix} \begin{bmatrix} S(TE1) \\ S(TE2) \\ S(TE3) \end{bmatrix} \right\|$$

$$\underbrace{\begin{bmatrix} T(x,y,TE_1) & T(x+1,y,TE_1) & \cdots \\ T(x,y,TE_2) & T(x+1,y,TE_2) & \cdots \\ T(x,y,TE_3) & T(x+1,y,TE_3) & \cdots \end{bmatrix}}_{T} = \underbrace{\begin{bmatrix} S(x,y,TE_1) & S(x+1,y,TE_1) & \cdots \\ S(x,y,TE_2) & S(x+1,y,TE_2) & \cdots \\ S(x,y,TE_3) & S(x+1,y,TE_3) & \cdots \end{bmatrix}}_{S} .* \underbrace{\begin{bmatrix} e^{-j2\pi\psi(x,y)TE_1} & e^{-j2\pi\psi(x+1,y)TE_1} & \cdots \\ e^{-j2\pi\psi(x,y)TE_2} & e^{-j2\pi\psi(x+1,y)TE_2} & \cdots \\ e^{-j2\pi\psi(x,y)TE_3} & e^{-j2\pi\psi(x+1,y)TE_3} & \cdots \end{bmatrix}}_{\Psi}$$

$$\begin{bmatrix} J(\psi(x,y)) & J(\psi(x+1,y)) & \cdots \end{bmatrix} = \left\| \left(I - AA\dagger\right) \underbrace{\begin{bmatrix} T(x,y,TE_1) & T(x+1,y,TE_1) & \cdots \\ T(x,y,TE_2) & T(x+1,y,TE_2) & \cdots \\ T(x,y,TE_3) & T(x+1,y,TE_3) & \cdots \end{bmatrix}}_{T} \right\|_{(x,x+1,\ldots)}$$

i. Vectorization Results

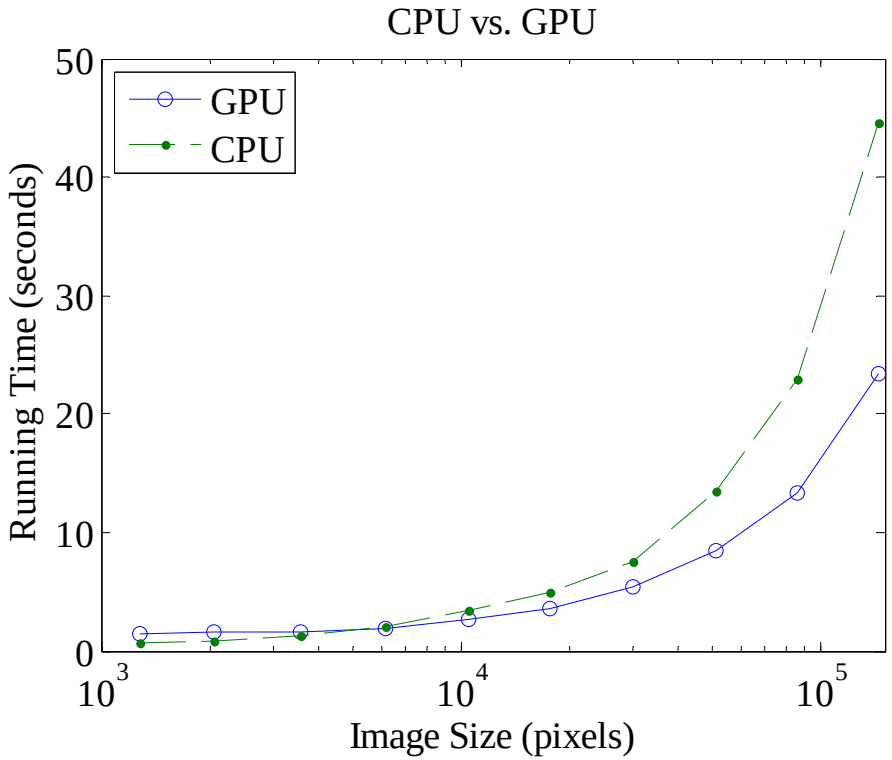

- 1000 iterations at fixed values of ψ on a 512x256x3 dataset
- GPU ~50% speedup relative to CPU (24 s vs 45 s)
- Images downsampled to determine break-even point (6000 pixels)
- Completely novel, MRI GPU-based reconstructions have only been done for non-cartesian k-space (ZP Liang at UIUC) and for k-t SENSE (Sorensen at CMIC in UK).

ii. Golden Section Search

- Idea: Start with a function f that has a minimum on the interval [a, b]. Choose two values x1, x2 with a < x1 < x2 < b, and then compare f (x1) and f (x2)

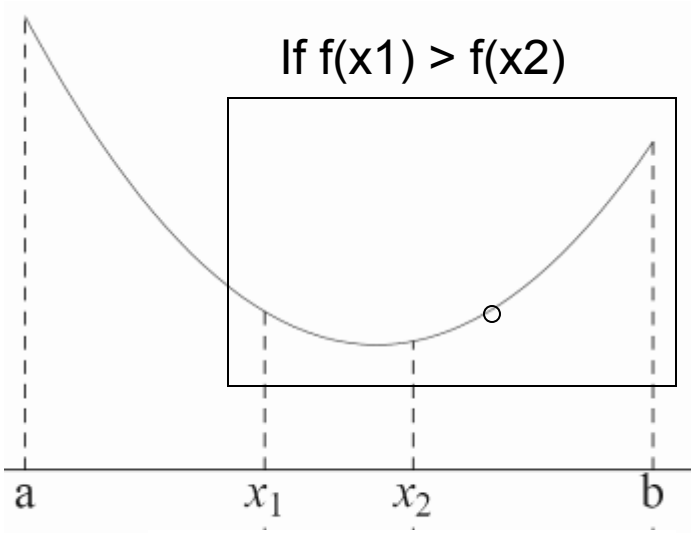

x2'=x2+(1+√5)/2*(b-x2)

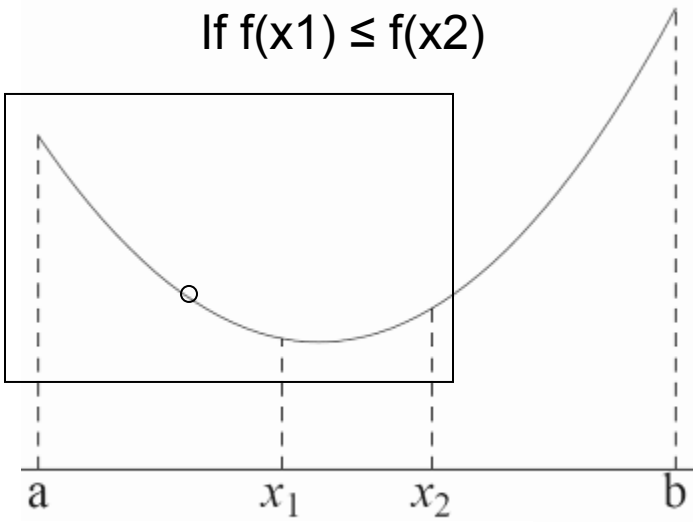

x1'=a+(1+√5)/2*(x1-a)

ii. Vectorized Golden Section Search

- The scalar algorithm only has three operations:
  - Evaluate F(x) where x is the new point to test
    - The new point is given by the golden ratio $(1+\sqrt{5})/2 \approx 1.61$
    - So the objective function must be able to evaluate multiple values of x independently and in parallel. Already done!
  - Compare F(x1) and F(x2)
    - In the scalar case, use an IF statement. In vectorized case, use **logical indexing** e.g. isLessThan = F(x1) < F(x2). isLessThan has one value for each entry in x1 which is 1 if the test was true and 0 if false. All IF statements are entirely replaced by logical indices.
  - Rearrange x1, x2, F(x1), F(x1) depending on the comparison
    - Use logical indexing operations in vectorized algorithm
    - b(isLessThan)=x2(isLessThan); x2(isLessThan)=x1(isLessThan); etc

ii. Brent's Method

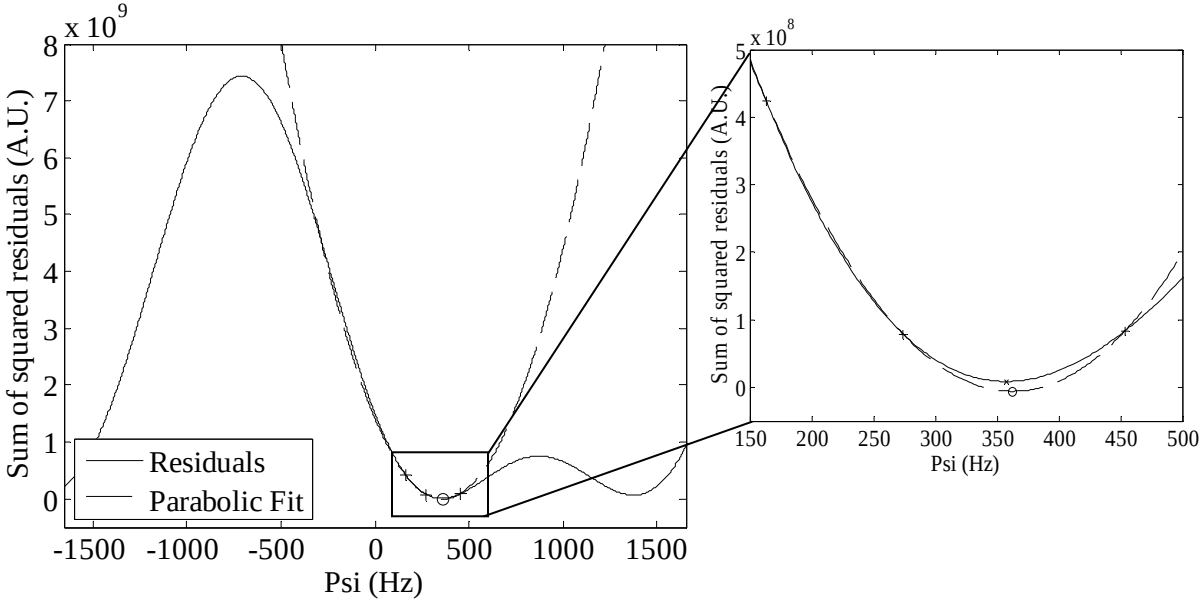

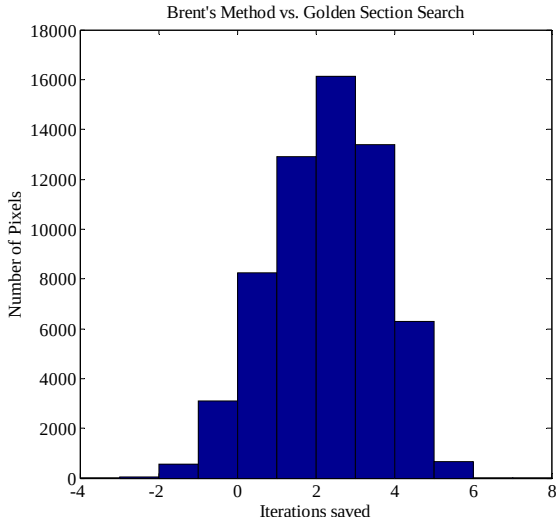

- Inverse parabolic interpolation is used to "jump" to the minimum of the residuals
- Brackets are maintained and used for golden sections if the parabolic fit is unacceptable (e.g. outside brackets, step size too small or too big, or a nonconvergent loop is detected).
- On average 3 fewer function evaluations than golden section search

iii. Unaliasing ψ

- Region growing algorithm initialized by operator (x_0, y_0)

For each (x,y) in SPIRAL(x_0, y_0)
  Fit 2D planar model to currently solved pixels around ψ(x,y)
  Extrapolate 10x10 neighborhood to get $\psi_P(x,y)$
  Compare $\psi_P(x,y)$ to ψ(x,y) and $\psi_1(x,y)$ +/- 1/ΔTE , +/- 2/ΔTE
  Assign ψ(x,y) as the minimum difference in the list
  Mark ψ(x,y) as solved

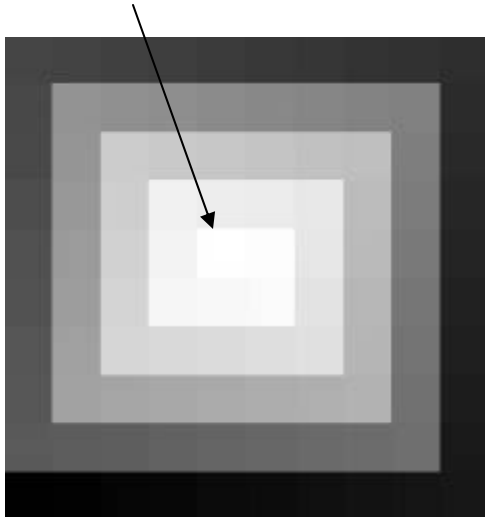

iii. Planar Extrapolation

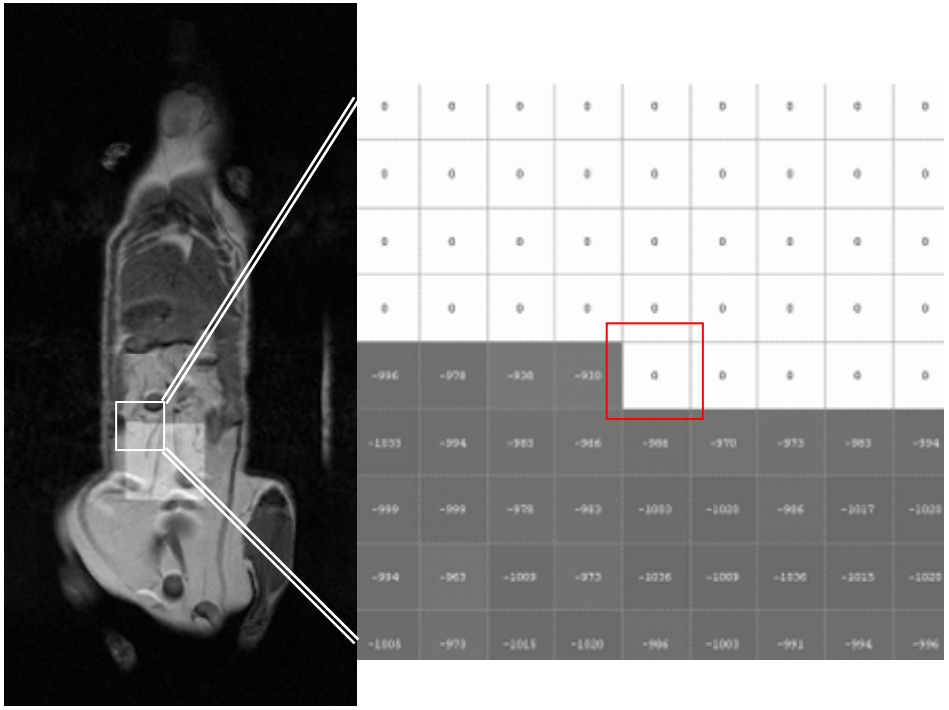

(a) (b)

$$W\begin{bmatrix}\psi(1,1)\\ \psi(2,1)\\ \psi(3,1)\\ \vdots\end{bmatrix} = W\begin{bmatrix}x(1,1) & y(1,1) & 1\\ x(2,1) & y(2,1) & 1\\ x(3,1) & y(3,1) & 1\\ \vdots & \vdots & \vdots\end{bmatrix}\begin{bmatrix}\psi_x\\ \psi_y\\ \psi_0\end{bmatrix}$$

If ψ_x or ψ_y > 150 Hz/pixel
Use weighted average
instead of extrapolation

Novel contribution: apply *a priori* knowledge to planar extrapolation model to prevent erroneous fitting

iii. Comparison of ψ unaliasing methods

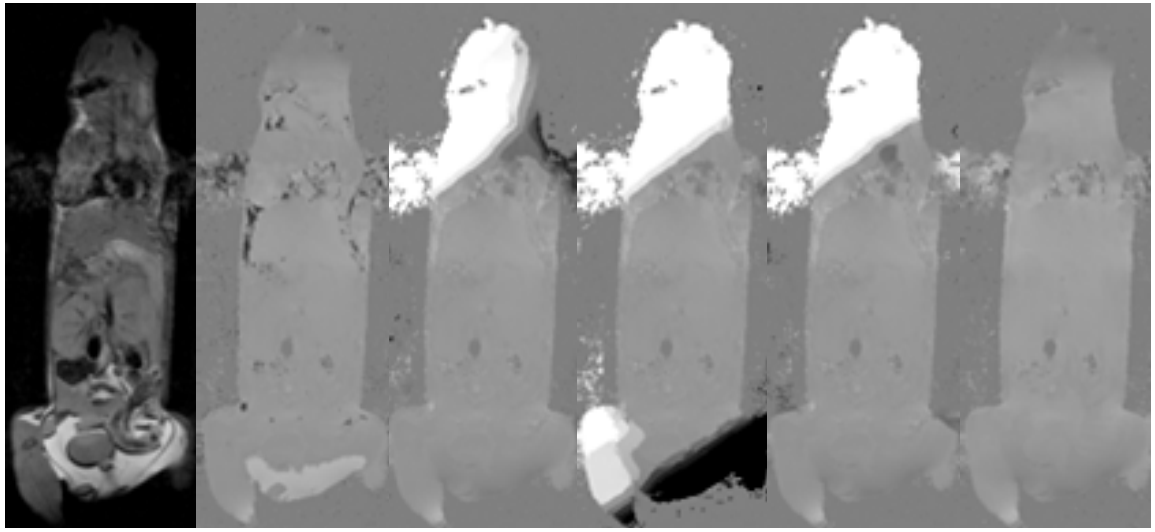

- New method (f) derives correct solution
- Literature methods (c)-(e) are incorrect

Aim #2 Conclusions

- Vectorized IDEAL equations are faster
- Iterations of the optimization are reduced by Brent's method
- Ψ aliasing is fixed using weighted planar extrapolation

Aim #3: IDEAL Mouse Imaging at 7T

- Hypothesis: IDEAL is more robust than CHESS for 7T mouse imaging in dietary obesity model
  i. IDEAL ratio images have better fat-water contrast than CHESS ratio images
  ii. IDEAL is more robust in the presence of field inhomogeneity
  iii. IDEAL accurately identifies phenotypes with lower errors than CHESS

IDEAL Imaging of a Mouse Model of Fatty Liver Disease at 7T

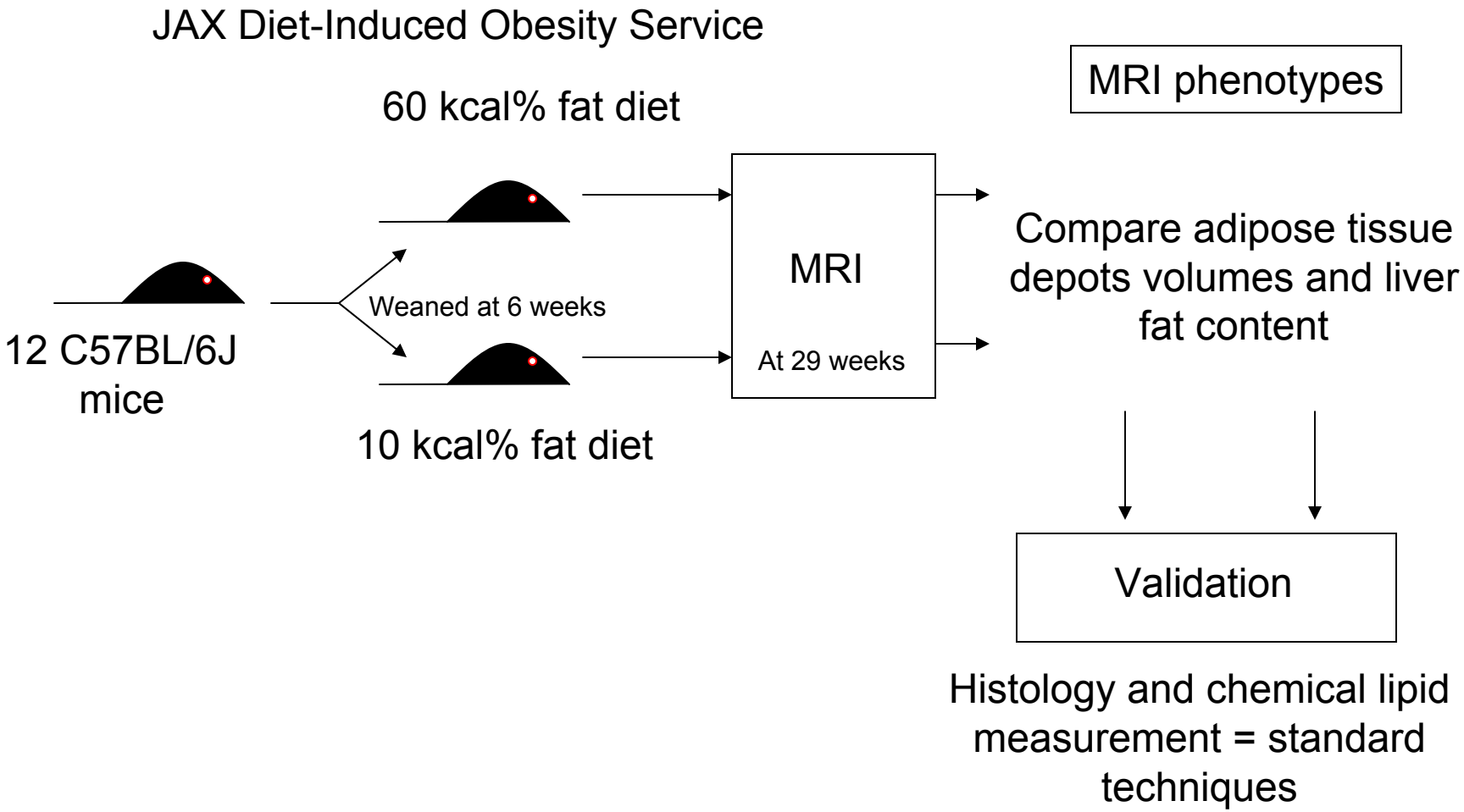

IDEAL Imaging of a Mouse Model of Fatty Liver Disease at 7T, images

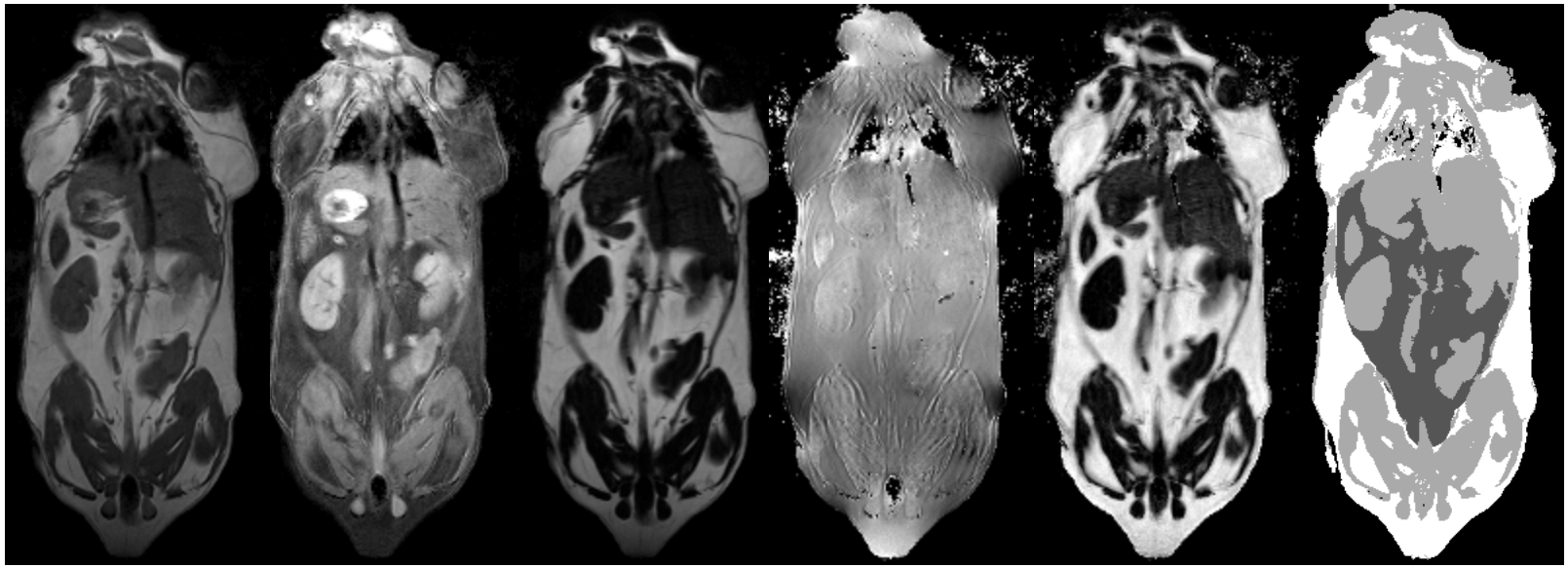

Input **|W|** **|F|** **ψ** **Ratio** **Label Image**

Visceral adipose tissue (dark gray): Ratio>0.50 and inside abdominal cavity
Non-visceral adipose tissue (white): Ratio>0.50 and outside abdominal cavity

The Ratio Image is used to create a Label Image, which is used to measure tissue volumes

i. Fat-Water Contrast to Noise Ratio

IDEAL

CHESS

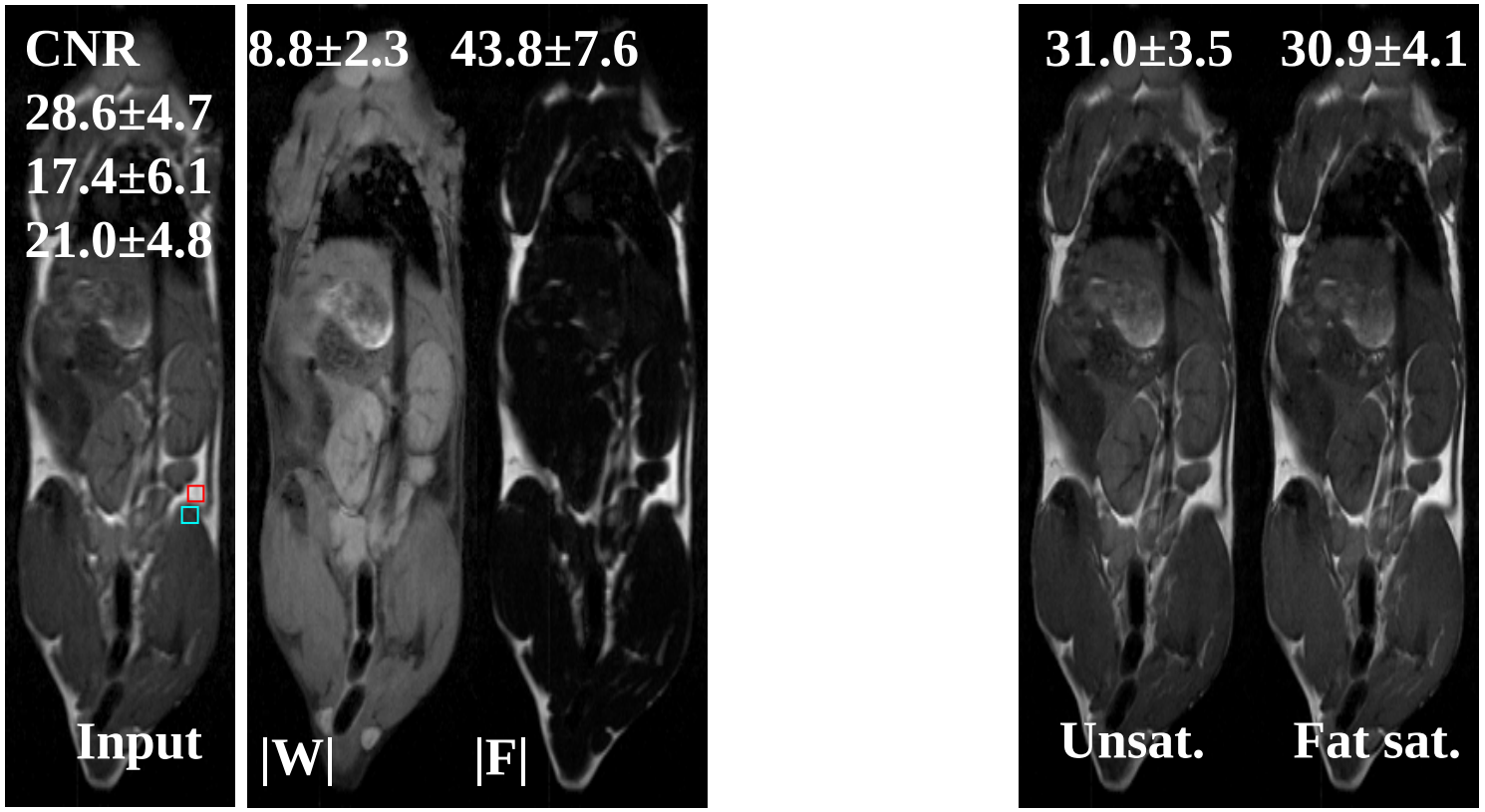

- IDEAL CNR is better than CHESS fat saturation
- CHESS suppression is unreliable

ii. Adipose Tissue Volume Phenotypes

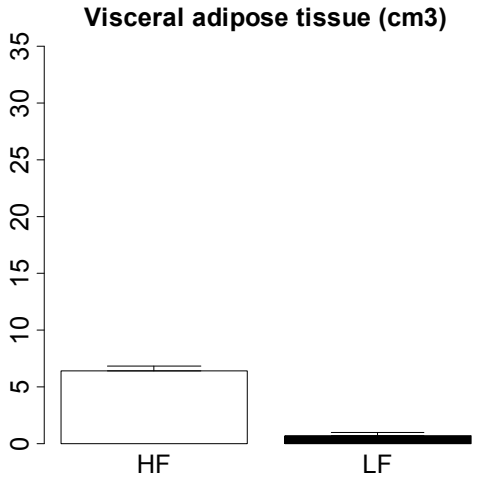

IDEAL

P<0.001

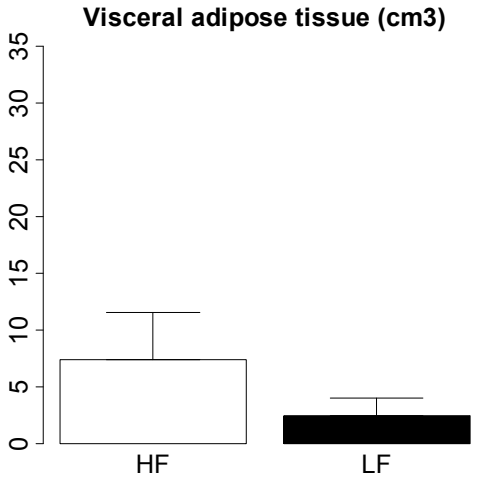

CHESS

P=0.02

Errors are smaller using IDEAL

ii. Adipose Tissue Volume Phenotypes, 2

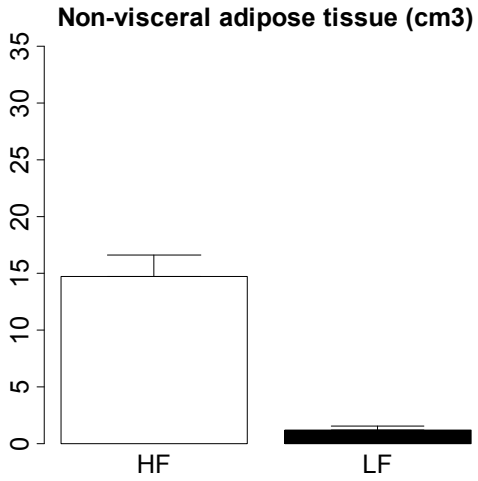

IDEAL

P<0.001

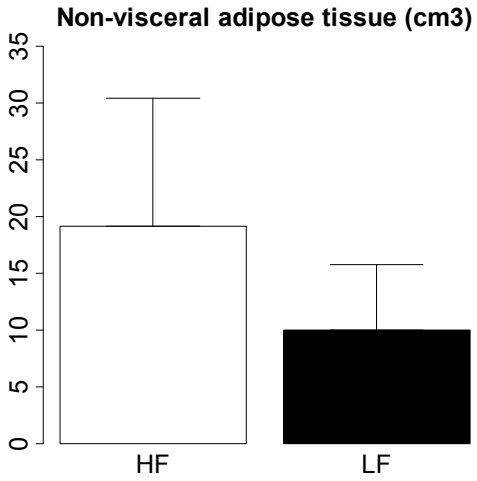

CHESS

P>0.10

CHESS is not even able to detect a statistically significant difference

iii. Identifying Phenotypes in Liver

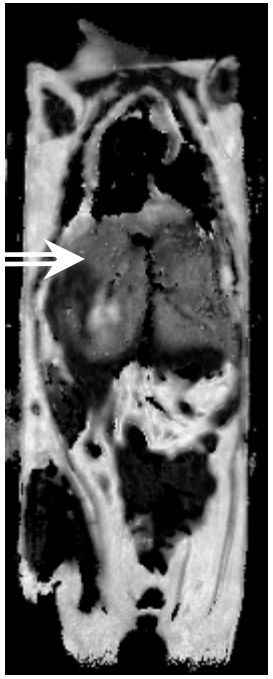

IDEAL ratio image

High fat diet mouse

Liver measurements

IDEAL: 27.2%±5.4%

CHESS: 37.2%±8.3%

Chemical lipid extraction:
220.6 mg triglyceride per g liver.

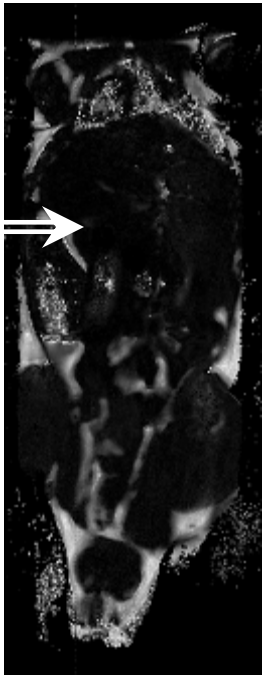

IDEAL ratio image

Low fat diet mouse

Liver measurements

IDEAL: 3.1%±1.7%

CHESS: 84.4%±15.2%

Chemical lipid extraction:
13.4 mg/g

iii. Liver Validation

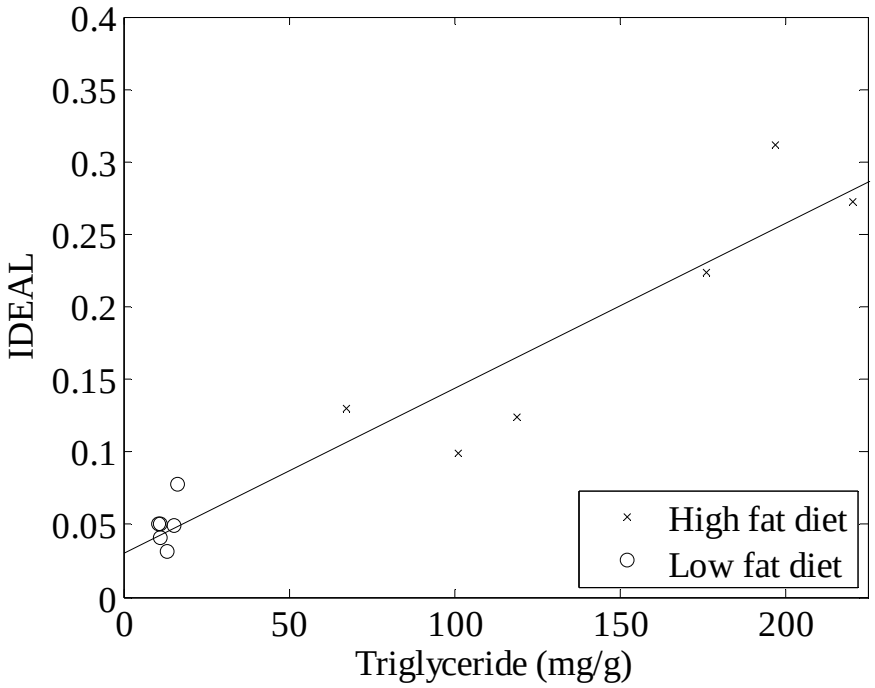

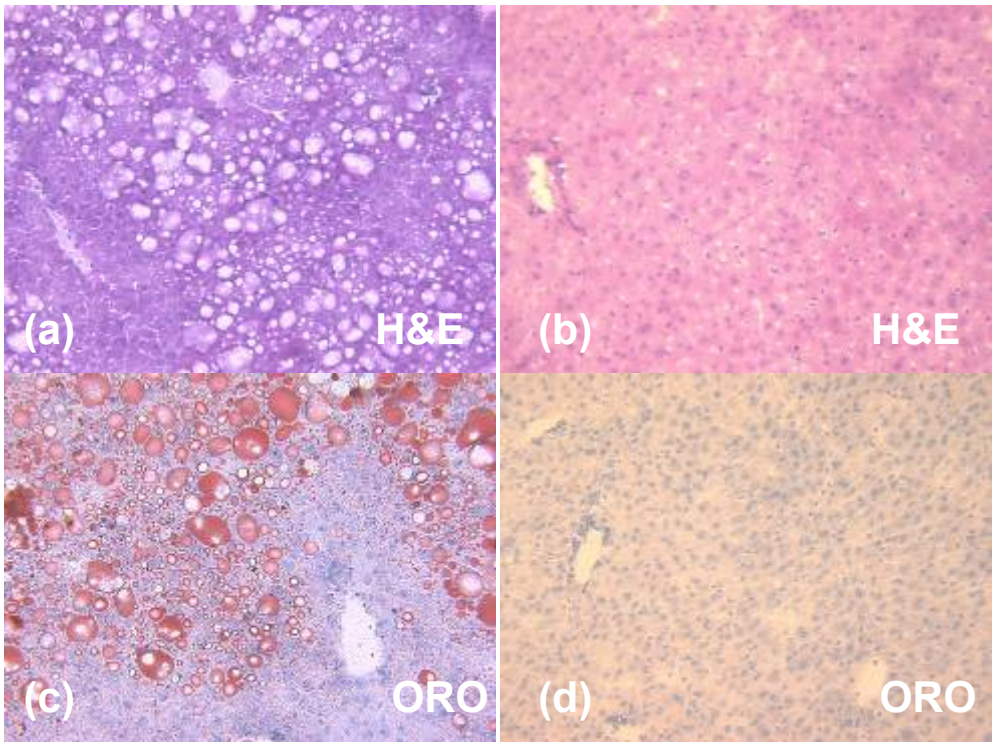

Chemical lipid extraction and histology agree with IDEAL measurements

Aim #3 Conclusions

- IDEAL is more robust than CHESS imaging
  - CNR is better
  - Handles wide range of B0 inhomogeneity
  - Standard deviation of tissue volume measurements were lower as measured by IDEAL than by CHESS in the mouse study

Conclusions

- Ratio imaging is a robust image analysis technique for phenotyping rodent models of obesity using MRI
- The ratio imaging technique was used for phenotyping rats on a clinical MRI scanner. MRI phenotypes included liver fat accumulation and enlarged visceral and subcutaneous adipose tissue depots.
- The IDEAL reconstruction was implemented on a graphics card with a 50% reduction in processing time
- The ratio imaging technique was validated using a mouse model of dietary obesity. Using IDEAL instead of CHESS imaging resulted in lower errors and more accurate measurements

Acknowledgements

- Thank you to:
  - My committee: Profs. David Wilson, Chris Flask, Xin Yu, Joseph Nadeau
  - The Biomedical Imaging Lab: Madhusudhana Gargesha, Donglai Huo, Daniel Izadnegahdar, Yuhao Jiang, Jun Miao, Sreenath Narayan, David Prabhu, Mohammed Qutaish, Debashish Roy, Grant Steyer, Olivier Salvado, Charlie Wang, and Patiwet Wuttisarnwattana
  - Research Collaborators and Associates: David Buchner, Colleen Croniger, Paul Ernsberger, Parvin Hakimi
  - My veterinary pathology consultant (and wife)
  - The entire staff of the Case Center for Imaging Research